

# Ammann Grid and Knot Structure of a Quasiperiodic Girih Pattern

Uli Gaenshirt

Sculptor & Researcher, Nuremberg, Germany; uli.gaenshirt@gmail.com

## Abstract

Girih patterns have been documented in the Orient since the early Middle Ages. They were generally constructed using geometric stencils. After discussing the quasiperiodic Penrose tilings from the 1970s and the corresponding covering models since the 1990s, appropriate Girih stencils were incorporated into a Penrose rhombus tiling. Subsequently, the resulting quasiperiodic Girih pattern was inserted into an Ammann grid-based covering cell. A very close agreement was found. Furthermore, it is shown that the Girih pattern is interwoven from closed knots of three different types, each of which has a one-to-one relationship with a single tile of the quasiperiodic HBS tiling. The Girih knots are discussed from different angles and illustrated in detail.

## Historical Introduction into Girih Patterns and Penrose Tilings

The geometric *Girih patterns* became established as decorations on religious buildings in the Middle East from the turn of the first millennium. Figure 1(a) shows a Girih stone relief from the *Hunat Hatun Complex* in Kayseri, Turkey, built in the early 13<sup>th</sup> century [16] (Photo: courtesy David Wade). The two highlighted shapes  $G_R$  and  $G_H$ , named after a rhombus and a hexagon whose internal angles are multiples of 36 degrees, represent the stencils with which the stonemason transferred the ornamentation outlined on the stencils onto the stone. Most of these patterns are periodic or adapted to the shape of the building.

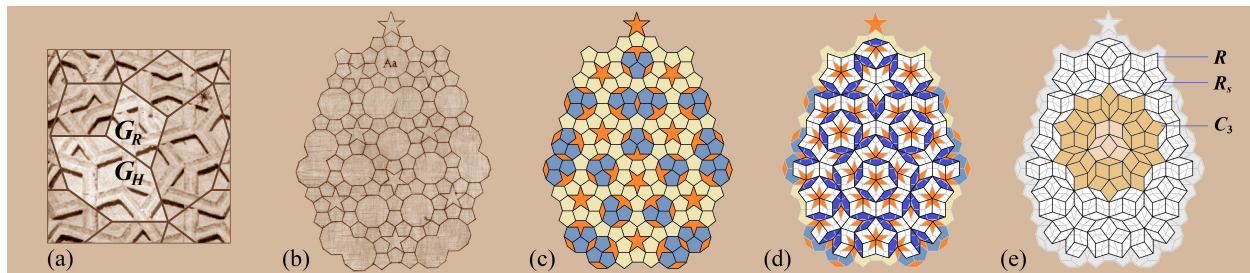


**Figure 1:** (a) *Girih stone relief from the Hunat Hatun complex in Kayseri, Turkey.* (b) *Kepler's copperplate Aa.* (c) *Penrose pentagon tiling PPT.* (d) *Penrose rhombus tiling P3 derived from the PPT.* (e) *Rhombus tiling with cartwheel  $C_3$ .* The Figures 1(c-e) and the Figures 2-8 are made by the author.

The Penrose tiles were developed by Roger Penrose (\*1931) in the 1970s to solve a mathematical tiling problem. He was inspired by the *copperplate Aa* [9] from Johannes Kepler (1571–1630). The original image (Figure 1(b), Photo: Université de Strasbourg) shows a pattern consisting in its central area of tiles with five-fold rotational symmetry, i.e. regular pentagons, decagons and pentagrams. Kepler used the example of the inevitably arising coupled decagons to show that a five-fold symmetry cannot exist in a periodic pattern. Penrose filled each single decagon of the *Aa* printing with three pentagons, one *boat* (a star with two missing spikes) and two *diamonds* (skinny rhombus) and let the coupled decagons *overlap* at a common diamond (Figure 1(c)). This tiling is known today as the *Penrose pentagon tiling (PPT or P1)*. A few years later Penrose derived two further tilings from the PPT, the *kite and dart tiling (P2)* and the *rhombus tiling (P3)*. The P3 tiling has only two *proto-tiles*, the *thick rhombus  $R$*  (acute angle 72 degrees) and the *skinny rhombus  $R_s$*  (acute angle 36 degrees). Figure 1(d) shows the equivalence relation of the PPT to the P3 tiling. The shape in the center of the P3 tiling in Figure 1(e) has an outline with ten-fold symmetry, which is absent in the inner structure. This arrangement is called the *cartwheel  $C_3$* .

## Specific Insights into Penrose Tilings, Ammann Bars and Associated Covering Models

Penrose developed two different rules for his tiles [11], which prevent periodic constellations and enforce quasiperiodicity, a prerequisite for the realization of a structural five-fold rotational symmetry. While the *matching rules* act locally, the *substitution rules* are global constructions. Both rules ensure that there are centers with five-fold rotational symmetry with different local ranges that are evenly distributed within a quasiperiodic (approximately periodic) arrangement.

### Matching Rules for Penrose Tiles and Covering Rules for Overlapping Quasi-Unit Cells

The matching rules prohibit *edge-to-edge constellations* of tiles that would allow periodicity. In the case of the Penrose rhombs in Figure 2(a), *Ammann line segments* are used as edge markers that guarantee quasiperiodicity [1][7]. The lines follow the path of a billiard ball entering and leaving the rhombus, perpendicular to a rhombus edge near an acute angle. In permissible arrangements, the Ammann line segments are straight lines and occur in five parallel families as shown in Figure 2(b). The space between two parallel Ammann lines is commonly called an *Ammann bar*. There are two types of Ammann bars. They are named after the intervals **L** (long) or **S** (short), which give their thickness. The ratio  $L/S$  is the *Golden Ratio*  $\tau = (\sqrt{5}+1)/2$ . Geometrically:  $\tau$  is the ratio of the diagonal of a pentagon to its edge length.

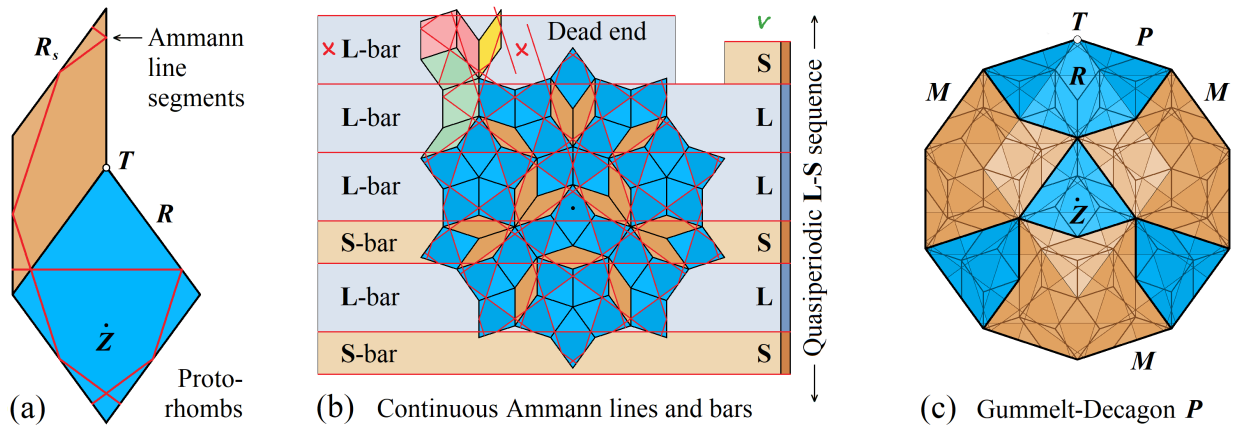


**Figure 2:** Matching rules: (a) Rhombs with Ammann line segments in permitted edge-to-edge relation. (b) Center: Fulfillment of the matching rules with continuous Ammann lines. Above: Incompleteness of the rules. (c) Gummelt-decagon  $P$  with three ochre subsets  $M$  and highlighted equivalent rhombus  $R$ .

The continuations of the line segments in the blue/ochre part in Figure 2(b) satisfy the matching rules. But the matching rules are incomplete. This means that following these rules does not protect against dead ends when puzzling tiles freely (Figure 2(b) above). The root cause is a violation of the *quasiperiodic L-S sequence*, which does not allow three consecutive **L**-bars. A more tricky case is illustrated in [6].

The sensational discovery of *quasicrystals* with five-fold rotational symmetry by Daniel Shechtman in 1982 [15] intensified the search for a *quasiperiodic unit cell*, comparable to *unit cells* in periodic crystals. The Penrose tilings have the disadvantage that they have at least two different cells. One of the first depictions of a *quasi-unit cell* can be found in Robert Ammann [1, p. 23], where he shows an arrangement of twelve identical *octagonal cells* that overlap in two different ways without changing their tile structure on the inside. See also [2] and [4]. The *Gummelt-decagon  $P$*  in Figure 2(c) is a *decagonal quasi-unit cell* introduced in 1996 [8].  $P$  has an equivalent relationship to the highlighted thick Penrose rhombus  $R$ . Consequently, the center  $Z$  and the top corner  $T$  of the decagon  $P$  can be transferred to the thick rhombus  $R$ . The *covering rules* of  $P$  require that the three ochre subsets  $M$  must be completely covered by the subsets  $M$  of overlapping cells [8][14]. The construction of  $P$  is based on the cartwheel  $C_3$  (see Figure 1(e) and 2(b)). Unfortunately, the covering rules of  $P$  have the same incompleteness as the matching rules of the Penrose tiles. Nevertheless, the concepts of the quasi-unit cells are very important.

### Substitution Rules for the Penrose Rhombus Tiling and for the Correlating Ammann Bars

During substitution, suitable building blocks are replaced by a specific arrangement of smaller copies. Tilings generated by substitution always fulfill the matching rules. Thus, substitution is the basis of all Penrose tilings. It reveals the hierarchical character of the tile order and makes it possible to create very large, error-free tile structures. In the following, the substitutions of Penrose rhombs and Ammann lines are described in detail and are illustrated in Figure 3(a-e). Finally, it is shown that a *self-similar Ammann subgrid* can be derived from the third step in the substitution of Ammann bars.

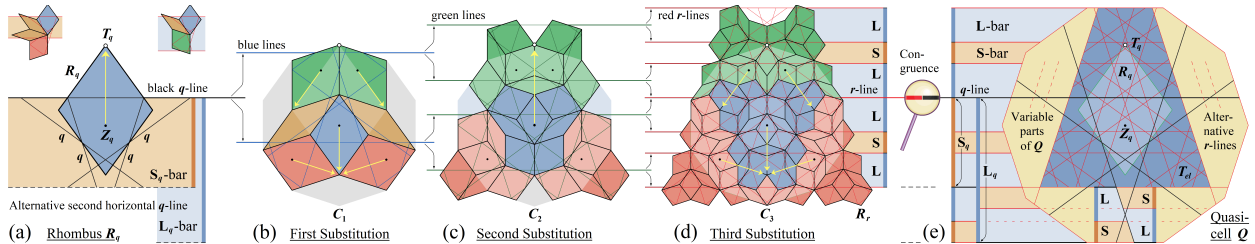


**Figure 3:** Substitution rules: (a) Thick rhombus  $R_q$  with  $q$ -lines and Ammann bars. (b) First substitution given by the orientation arrows. (c) Second substitution. (d) Third substitution with gapless decagon  $C_3$ . (e) Quasi-cell  $Q$  with the elementary trapezoid  $T_{el}$ . (a-e) Substitution of the horizontal Ammann lines.

The thick rhombus  $R_q$  in Figure 3(a) has five fixed black  $q$ -lines, which are arranged in the same way as the red lines in Figure 2(a). The subscript  $q$  refers to the fixed size of  $R_q$  which is determined by the equivalent relationship of  $R_q$  to the grid-based *quasi-cell*  $Q$  (Figure 3(e)). The sketches in Figure 3(a) above show how the alternative position of a second horizontal  $q$ -line depends on the constellations of neighboring rhombs. The orientation of  $R_q$  is marked by a yellow arrow pointing from  $Z_q$  to  $T_q$ . The five thick rhombs in Figure 3(b) are scaled down with the substitution factor  $1/\tau$  and are then transformed according to the *orientation arrows*. Together with the two additional ochre skinny rhombs, they represent the *first substitution*. The identically formed *cartwheel*  $C_1$  is a tile-based quasi-unit cell. The undefined grey areas complement  $C_1$  to form a decagon. The two horizontal blue Ammann lines of  $C_1$  are not congruent with the black Ammann line ( $q$ -line) from  $R_q$  in Figure 3(a). The *second substitution* in Figure 3(c) is an *iteration* of the first. Here  $C_1$  is contracted and transformed according to the orientation arrows in Figure 3(b). The green Ammann lines are neither congruent with the blue Ammann lines of  $C_1$ , nor with the red  $r$ -lines in Figure 3(d). The trapezoidal *third substitution* in Figure 3(d) is the *second iteration* of the first substitution and contains the gapless *cartwheel decagon*  $C_3$ , which is made by reduced rhombs  $R_r = R_q/\tau^3$  and  $R_{rs} = R_{qs}/\tau^3$  (the index  $r$  stands for “reduced” and  $s$  for “skinny”). Through the magnifier between the Figures 3(d) and 3(e) it can be obtained that the horizontal black  $q$ -line of the thick rhombus  $R_q$  is congruent with the red  $r$ -line between two neighboring L-bars. The blue *elementary trapezoid*  $T_{el}$  in Figure 3(e) shows that this is also true for the other four  $q$ -lines. This means that each  $q$ -line is an  $r$ -line of higher level, since the  $L_q$ - and  $S_q$ -bars contain integer numbers of L- and S-bars. Because of this partial congruence, the three-step-substitution is called the *concordant substitution of Ammann bars* [3], written as:  $L_q \rightarrow \text{LSLSL}$  and  $S_q \rightarrow \text{LSL}$ . The substitution factor is  $1/\tau^3$ . It follows that the  $r$ -line grid (L-S grid) is a self-similar subgrid of a  $q$ -line grid ( $L_q$ - $S_q$  grid).

### Overlapping Quasi-Cells $Q$ as the Basic Building Blocks of a Growth Algorithm

The *Quasiperiodic Succession Algorithm*, published in 2007 [3], is a *growth algorithm* [3][4][5]. It works locally like the matching rules, but just like the substitution rules, it generates a very large error-free cartwheel-type tiling  $C_n$  by controlled overlaps of quasi-cells  $Q$  that are based on the Ammann grid (see Figure 3(e)). Inside  $Q$  is the elementary trapezoid  $T_{el}$  which, because  $T_{el}$  is a quasi-unit cell, completely covers the plane in regular arrangements. However, as  $Q$  is larger than  $T_{el}$ ,  $C_3$  and  $P$ , it has an area outside  $T_{el}$  that is only defined when  $Q$  is completely covered by other cells. Therefore  $Q$  is called a quasi-cell and not a quasi-unit cell! The Ammann grid of  $Q$  has a strong correspondence to a *quasiperiodically modified Girih pattern*, which will be developed in the following section.

## A Medieval Islamic Girih Pattern from Kayseri and its Quasiperiodic Modification

In 2007, P. J. Lu and P. J. Steinhardt published one of the first articles on the relationship between Islamic Girih patterns and Penrose tilings [10]. Among the numerous articles from subsequent years on this topic, I would like to highlight a 2022 paper by J. E. Padilla [12], in which she demonstrates how *traditional decagonal Islamic motifs* can be incorporated into a Penrose pentagon tiling PPT (see Figure 1(c)). Please also note the references therein, which lead to further interesting articles on this topic.

The motif that gave the inspiration for the present work is a Girih stone relief from the *Hunat Hatun Complex* in Kayseri, Turkey, built in the 13<sup>th</sup> century [16]. The relief is the lateral decoration of a portal. The motif on the relief strip is periodic, as can be seen from the vertically repeating green and red sequences in Figure 4(a). This topic is discussed in [13] (in German). See also the Kayseri pdf in [5].

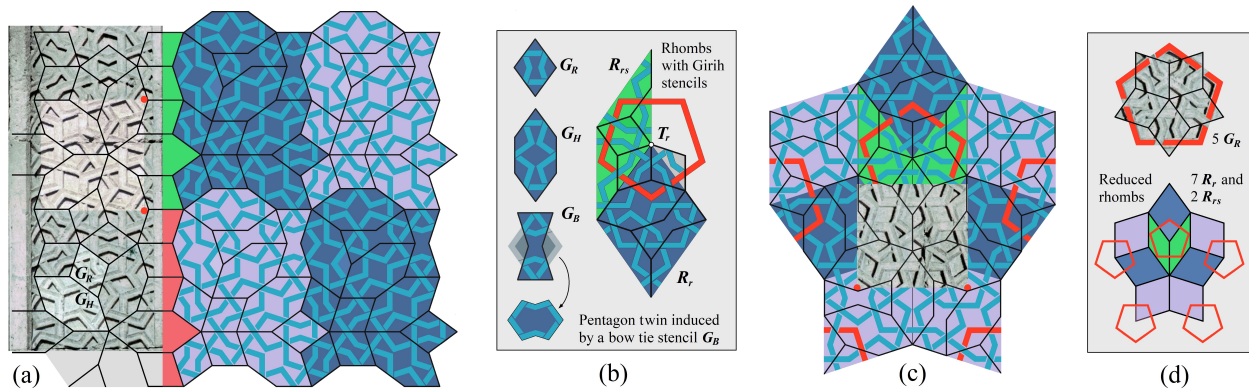


**Figure 4:** (a) Left: Photo of the ancient periodic Kayseri Girih pattern with Girih stencils superimposed. Right: Girih pattern with two periods. (b) Left: Girih stencils  $G$ . Right: Penrose rhombs  $R_r$  and  $R_{rs}$  with incorporated Girih stencils. (c) Quasiperiodic Girih pattern with inserted detail from the original relief. (d) Above: Red Girih pentagon with inserted detail from the original. Below: Sketch of Figure 4(c).

In the left part of Figure 4(a), two types of historical *Girih stencils* are superimposed on the photo of the original relief. One type has a rhombic shape ( $G_R$ ), the other type has the shape of an elongated hexagon ( $G_H$ ). The right part of Figure 4(a) shows four unit cells of a similar periodic Girih pattern. This pattern has the same vertical period as the Kayseri pattern, but there is also a horizontal period, so the pattern can be extended as desired. In addition, a third historical Girih stencil is used ( $G_B$ ), which has the shape of a *bow tie*. The three stencil types are shown separately on the left side of Figure 4(b).

On the right side of Figure 4(b), the Girih stencils are fitted into the thick rhombus  $R_r$  and the skinny rhombus  $R_{rs}$ . Each thick rhombus contains one-fifth of a closed red Girih pentagon, and each skinny rhombus contains two-fifths of it. Figure 4(c) shows an arrangement of nine Girih-patterned rhombs. In its center a section of the original periodic stone relief is inserted (rotated 90 degrees clockwise), without contradicting the quasiperiodic pattern. In Figure 4(d) above, another section of the original relief is fitted into one of the numerous red Girih pentagons. Below there is a reduced sketch of the pattern shown in Figure 4(c) to clarify the rhombus arrangement behind the photo inserted there.

We can note that the quasiperiodic Girih pattern in Figure 4(c) is very similar to the original relief and differs from it mainly by the absence of the periodic pattern repetition and by the additional existence of *pentagon twins* (Figure 4(b) below). These twins, induced by the bow-tie stencils  $G_B$ , can also be seen in the periodic pattern on the right side of Figure 4(a). There, however, the pentagon twins have only two different alignments, whereas in the quasiperiodic pattern in Figure 4(c) they appear in each of the five possible orientations. An approximately uniform distribution of the different orientations of shapes without their own five-fold rotational symmetry is an essential characteristic of a structural five- or ten-fold symmetry, which can also be found in naturally grown quasicrystalline nuclear structures.

## The Correlation of the Modified Girih Pattern with the Ammann Grid of the Quasi-Cell $Q$

Figure 5(a) shows the quasi-cell  $Q$  with the five black  $q$ -lines, that are firmly connected to  $R_q$ ,  $T_{el}$  and  $Q$ . The light blue rhombus  $R_q$  thus has an equivalence relation to  $Q$ . The five red twin-scales  $I$  control the growth process of the overlapping quasi-cells  $Q$ . The twin-scales are delimited by red  $r$ -lines. That makes it clear that the Ammann grid is the basis of the growth algorithm. The five scale-values of a cell  $Q$  are transferred to the twin-scales  $I$  of all possible overlapping cells. Each overlap in which this results in five valid values is permissible. More information on the growth algorithm can be found in the supplement.

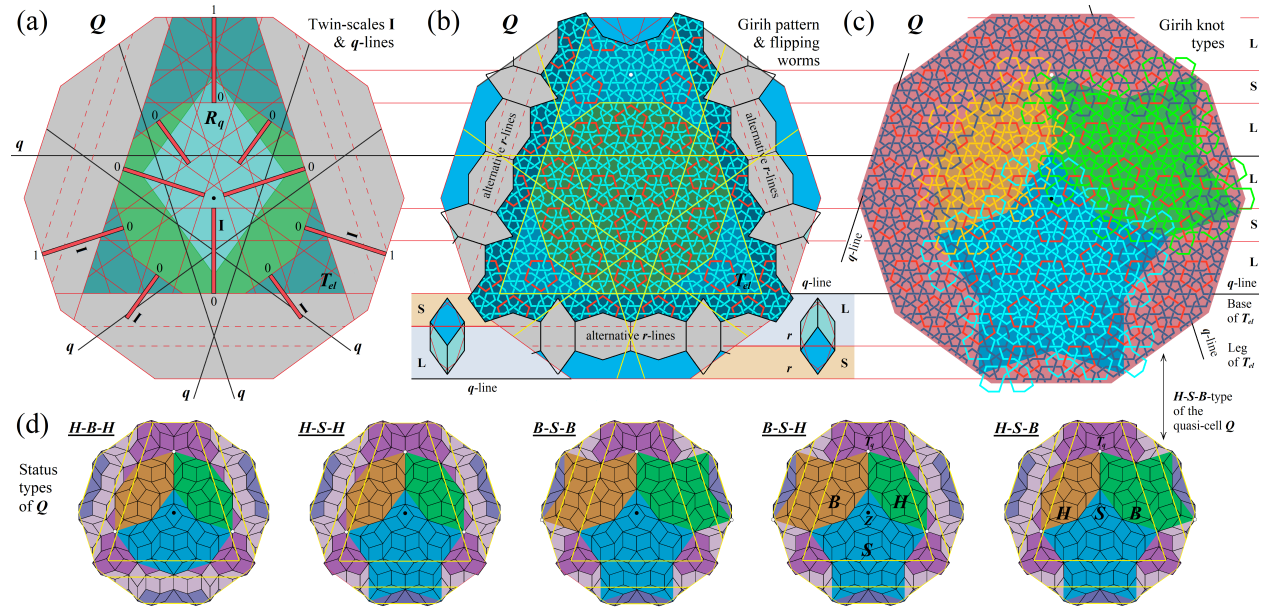


**Figure 5:** (a) Quasi-cell  $Q$  with five red twin-scales and five  $q$ -lines. (b)  $Q$  with Girih pattern and three grey flipping worms. (c)  $Q$  with three distinct Girih knot types  $H$ ,  $S$  and  $B$ . (d) The five status types of  $Q$ .

Figure 5(b) shows the correspondence between the quasiperiodic Girih pattern and the Ammann grid of the quasi-cell  $Q$ . The pattern is generated by replacing the rhombus  $R_q$  with the reduced rhombs  $R_r$  and  $R_{rs}$  of the third substitution (Figure 3(d)). These rhombs are in turn replaced by a Girih pattern fitted into the reduced rhombs, as shown in Figure 4(b). The correspondence between the Girih pattern and the Ammann grid is very close. Ammann lines which represent structural elements of  $Q$  are highlighted in yellow here. Three quarters of each  $r$ - or  $q$ -line correspond to rectilinear segments of the Girih pattern! The rhombus positions in the three grey worms are undefined as long as no cell overlap has taken place. The two elongated hexagons next to the lower worm show that the horizontal red  $r$ -line changes the dashed variant when the rhombs are flipped. Consequently, the corresponding black  $q$ -line also changes its position from an edge of  $T_{el}$  to a parallel edge of  $Q$  or vice versa (see also Figure 3(e) below).

In Figure 5(c), the first *alternative*  $q$ -line lies on the base of  $T_{el}$ . The second alternative  $q$ -line is on the right leg of  $T_{el}$ . The third alternative  $q$ -line lies on the edge of  $Q$  which is parallel to the left leg of  $T_{el}$ . These three  $q$ -lines define the entire Girih pattern within the quasi-cell  $Q$ ! Surprisingly, three closed *Girih knots* can now be found, which become visible through different coloring (The term "Girih knot" here refers to a closed (mathematical) knot within the Girih wickerwork). Each knot has a relationship to a geometric tile in the background: the yellow knot to a hexagon  $H$ , the green knot to a boat  $B$  and the blue knot to a star  $S$ . These three tiles are the proto-tiles of the *HBS tiling* [14]. Please note: the boat and the star of the *HBS tiling* have another shape than the skinny versions of the PPT (see Figure 1(c)).

Figure 5(d) shows the five status types of  $Q$ . Mathematically, eight ( $2^3$ ) types would be possible, but three of them lead to contradictions. The types are named in tile order from left (yellow) to bottom (blue) to right (green). Consequently, the status type in Figure 5(c) is denoted as the *H-S-B type* of  $Q$ .

### The HBS Tiles Created by Overlaps of $C_1$ and the Girih Knots Created by Overlaps of $T_{el}$

Figure 6(a-c) shows that the *HBS*-tiles can be easily composed of Penrose rhombs by overlapping cartwheels  $C_1$  (see Figure 3(b)). In Figure 6(a) the coverage areas are the thick rhombs, labeled with  $H$ . Together with their two neighboring skinny rhombs they form the yellow and the two green hexagons  $H$ . In Figure 6(b), the covered rhombus ( $B$ ) forms the green boat  $B$  together with one skinny and two thick rhombs. In Figure 6(c), the covered rhombus ( $S$ ) and four thick rhombs form the blue star  $S$ .

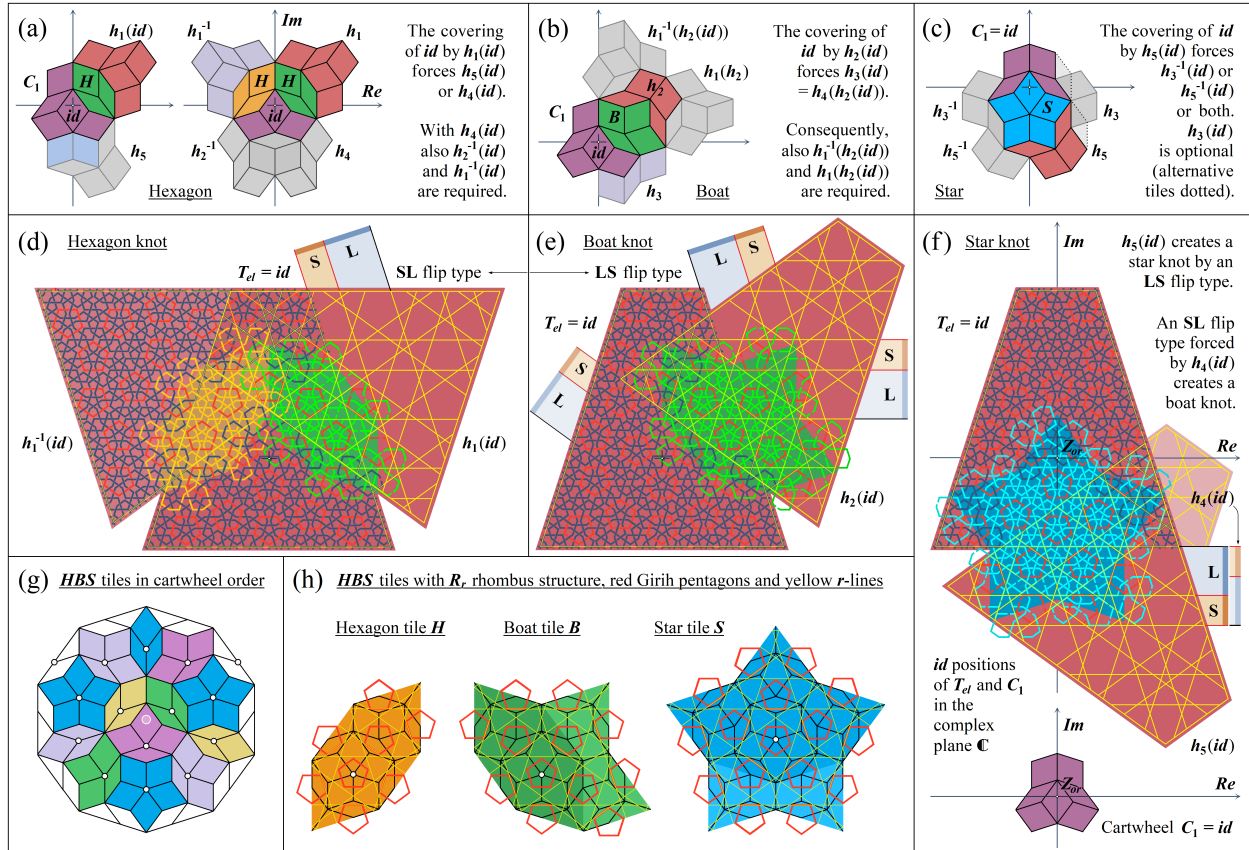


**Figure 6:** Generation of *HBS* tiles by  $C_1$ : (a)  $H$  tile, (b)  $B$  tile, (c)  $S$  tile. Generation of Girih knots by  $T_{el}$ : (d)  $H$  knot, (e)  $B$  knot, (f)  $S$  knot. (g) *HBS* tiling in a cartwheel arrangement. (h) Decorated *HBS* tiles.

In Figure 6(d-f), the three Girih knots are generated by the same coverings as the *HBS* tiles before, except that now the trapezoids  $T_{el}$  are overlapped and mathematical terms are used to describe them. The yellow  $H$  knot is part of the overlapping Girih structures of the trapezoids  $id$  and  $h_1^{-1}(id)$ . The green  $H$  knot shows the correlation of the Girih structure of the trapezoid  $id$  with the yellow  $r$ -line grid of the trapezoid  $h_1(id)$ . Figure 6(e) illustrates the overlap of the trapezoid  $id$  with  $h_2(id)$ . Please compare: While the **SL** flip type in Figure 6(d) creates the green  $H$  knot, the inverse **LS** flip type in Figure 6(e) creates the green  $B$  knot! The overlap of the trapezoid  $id$  with  $h_5(id)$  in Figure 6(f) creates the blue  $S$  knot. The  $id$  positions of  $T_{el}$  and  $C_1$  in the complex plane  $\mathbb{C}$  with  $Z_{or}$  at the origin allow the mathematical definition of the transformations  $h_i(id)$  and their inverses  $h_i^{-1}(id)$ , with  $i = \{1, 2, 3, 4, 5\}$ . For details see [8] p. 7.

Figure 6(g) shows an *HBS* tiling in a  $C_3$  cartwheel arrangement. The colors are chosen so that same colors do not touch at all, not even across corners. Corresponding Girih knots in similar colors can be seen in Figure 8 (please note the cartwheel center in the lower middle of Figure 8). In Figure 6(h), the *HBS* tiles are composed of reduced rhombs  $R_r$  and  $R_{rs}$  (see Figure 5(d)) decorated with yellow  $r$ -lines and red Girih pentagons. The highlighted sections indicate that an  $S$  tile contains a  $B$  tile and a  $B$  tile contains an  $H$  tile. The white dots are the centers of the local five-fold rotational symmetry (compare Figure 8).

### Knot Components as Basic Building Blocks of the Three Girih Knot Types

To understand how the Girih knots create a uniform pattern, the components of each knot must be studied. In Figure 7(a), the  $H$  knot is shown against the background of a hexagon  $H$  consisting of one thick and two skinny rhombs. The dendritic Girih component, here colored black, consists of five identical Girih meanders interwoven into a five-fold rotational symmetry. Eight of its ten ends are connected by four small loops (blue and yellow) and two ends are connected by one large loop (green). In Figure 7(b), two of the small loops are removed together with the corresponding skinny rhombus. In Figure 7(c), two thick rhombs are fitted into the resulting gap. The associated large loops create a  $B$  knot! An  $S$  knot is formed when all four small loops in Figure 7(a) are replaced by four large loops. In Figure 7(d), another skinny rhombus is added to the right of the created  $B$  knot. The two corresponding small loops (yellow and green) complete the Girih structure between the two centers with five-fold symmetry (white dots).

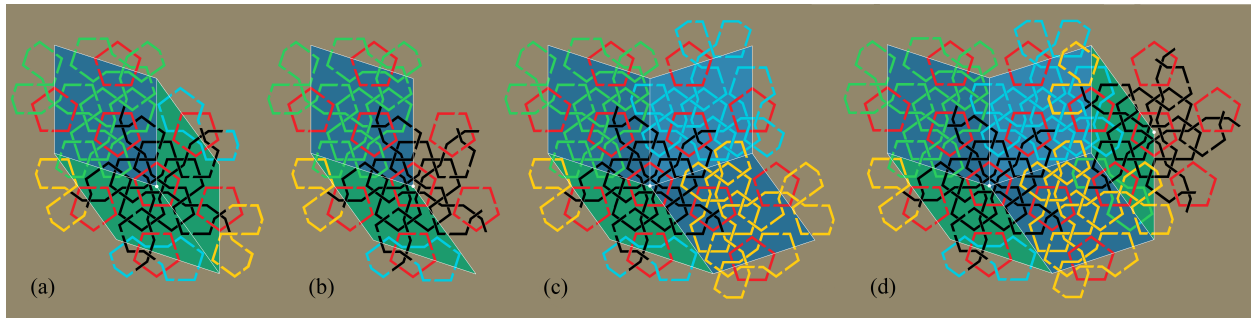


**Figure 7:** (a) Components of the  $H$  knot. (b) Pruned  $H$  knot. (c) Components of the  $B$  knot. (d)  $B$  knot with skinny rhombus on the right side including corresponding loops and second center of symmetry.

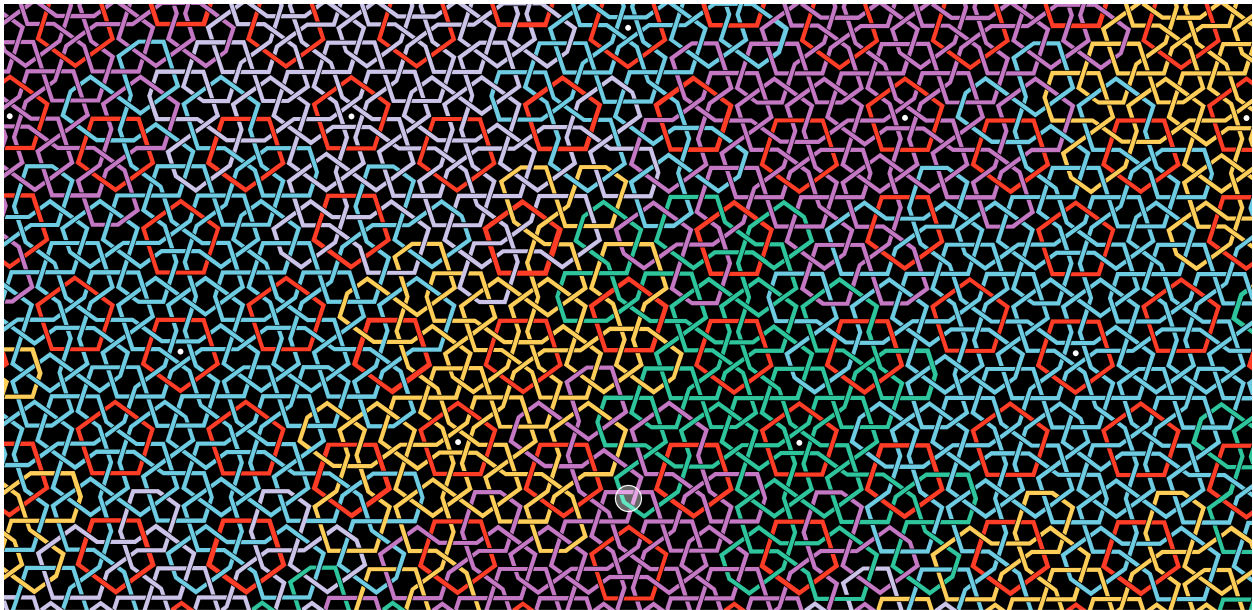


**Figure 8:** Uniform quasiperiodic Girih pattern consisting of differently colored Girih knots.

The Girih knot structure in Figure 8 is based on the  $HBS$  cartwheel  $C_3$  in Figure 6(g). Its center is located in the white circle in the lower middle. The nine white dots are the centers of five-fold symmetry and correspond to the nine dots in the upper half of Figure 6(g). Eight of the spaces between two white dots have the same structure as in Figure 7(d). However, while there each knot component has a distinct color, in Figure 8 each Girih knot has its own color, which matches the color of the corresponding  $HBS$  tile in Figure 6(g). Together with their mutual interweaving, the colorful knots create a picturesque image.

## Summary, Conclusion and Outlook

Inspired by a 13<sup>th</sup>-century Girih stone relief, a similar but quasiperiodically modified Girih pattern was created by fitting historical Girih stencils into the quasiperiodic Penrose rhombs. We found a very strong correlation of the resulting Girih knots with the HBS-tiling and the Ammann bar grid of the quasi-cell  $Q$ . Due to the fact that the Girih segments are angled at 36 or 72 degrees and due to their incorporation into the Penrose rhombs, it is clear that they are divided into the five possible orientations, each with a share of 20%. This means that the quasiperiodic Girih pattern can be understood as a quasicrystalline structure. By mirroring of certain stencil positions within the rhombs, the Girih knots can be entirely altered. Such variations hold a great potential for a deeper understanding of the quasiperiodic Girih patterns.

## Acknowledgements

Thanks to my friend Michael Willsch for the help he has given me in the past. Thanks to the imaginary-team for making my galleries, exhibitions and files available. Thanks to deepl for language optimization. Thanks to Helena Verrill. I would like to dedicate this work to Professor Shelomo Ishaq Ben-Abraham.

## References

- [1] R. Ammann, B. Grünbaum, G. Shephard. "Aperiodic Tiles." *Discrete & Comp. Geometry*, vol. 8, 1992, p. 23. <https://link.springer.com/content/pdf/10.1007/BF02293033.pdf>
- [2] S. I. Ben Abraham, F. Gähler. "Covering cluster description of octagonal MnSiAl quasicrystals." *Physical Review*, vol. B 60, 1999, pp. 860–864.
- [3] U. Gaenshirt, M. Willsch. "The local controlled growth of a perfect Cartwheel-type tiling called the Quasiperiodic Succession." *Philosophical Magazine*, vol. 87, 2007, pp. 3055–3065. <https://hal.science/hal-00513832>
- [4] U. Gaenshirt, M. Willsch. "Octagonal Type of the Quasiperiodic Succession Algorithm." *Materials Structure*, vol. 22, 2015, pp. 299–300. [https://www.imaginary.org/sites/default/files/octqusucc\\_poster.pdf](https://www.imaginary.org/sites/default/files/octqusucc_poster.pdf)
- [5] U. Gaenshirt. "Quasicrystalline Wickerwork." *Imaginary Gallery*. <https://www.imaginary.org/gallery/quasicrystalline-wickerwork>
- [6] U. Gaenshirt. "Devilline's Talk." *Bridges 2024 Conference Art Exhibition, 2024*. <https://gallery.bridgesmathart.org/exhibitions/bridges-2024-exhibition-of-mathematical-art/uli-gaenshirt>
- [7] B. Grünbaum, G. C. Shephard. "Tilings and Patterns." *W. H. Freeman*, 1987, pp. 571 ff.
- [8] P. Gummelt. "Penrose tilings as coverings of congruent decagons." *Geometriae Dedicata*, 62, 1996, pp. 1–17.
- [9] J. Kepler. "Harmonices Mundi / Liber II." *Ioannes Plancus*, 1619, pp. 47–66. <https://www.digitale-sammlungen.de/de/view/bsb10860898?q=%28harmonices+mundi&page=98,99>
- [10] P. J. Lu, P. J. Steinhardt. "Decagonal and Quasi-Crystalline Tilings in Medieval Islamic Architecture." *Science*, 315, 2007, pp. 1106–1110. <https://www.science.org/doi/10.1126/science.1135491>
- [11] R. Penrose. "Pentaplexity A Class of Non-Periodic Tilings." *Mathematical Intelligencer*, 2, 1979, pp. 32–37.
- [12] J. E. Padilla. "Penrose Tiling Arrangements of Traditional Islamic Decagonal Motifs." *Proceedings of Bridges 2022*, 2022, pp. 143–150. <https://archive.bridgesmathart.org/2022/bridges2022-143.html>
- [13] C. Pöppe. "Nichtperiodische Parkettkunst." *Spektrum der Wissenschaft*, 19/7, 2019, pp. 80–84.
- [14] M. Reichert, F. Gähler. "Cluster model of decagonal tilings." *Physical Review*, vol. B 68, 2003, pp. 1–10. <https://www.math.uni-bielefeld.de/~gaehler/papers/PRB14202.pdf>
- [15] D. Shechtman et al. "Metallic Phase with Long-Range Orientational Order and No Translational Symmetry." *Physical Review Letters*, 53, 1984, pp. 1951–1953. <https://journals.aps.org/prl/pdf/10.1103/PhysRevLett.53.1951>
- [16] D. Wade. "Pattern in Islamic Art." *The Wade Photo Archive / Turkey / Kayseri / Hatuniye complex / TUR 0731*. [https://patterninislamicart.com/s/collections/main-archive/piia\\_image/tur0731](https://patterninislamicart.com/s/collections/main-archive/piia_image/tur0731)